PRAMANA
— journal of
physics

QCD results from HERA and JLAB

KATJA KRÜGER[a,*]
[a]Kirchhoff Institut für Physik, Universität Heidelberg, Germany

Abstract. Recent QCD results from electron-proton interactions at HERA and JLAB are presented. Inclusive cross section measurements as well as studies of the hadronic final state like jet production or the production of heavy quarks are discussed. The results are compared to perturbative QCD predictions and their impact on the determination of the parton density functions of the proton as well as of the strong coupling α_s is discussed.

Keywords. electron proton scattering, QCD, PDFs, jets

PACS Nos. 12.38.Qk, 13.60.Hb, 13.87.-a, 13.88.+e

1. Introduction

Electron [1] proton scattering offers unique possibilities to study the structure of the proton in a clean experimental environment. The exchanged virtual boson, a photon, a Z or a W boson, acts as a probe of the internal structure of the proton. The resolving power is given by the virtuality Q^2 of the exchanged boson. The kinematics of the interaction are further described by the inelasticity y, which corresponds to the relative energy transfer from the electron to the boson in the proton rest frame, and the Bjorken scaling variable x which, in the Quark Parton Model, corresponds to the fraction of the proton momentum carried by the struck quark. These variables are connected with the electron proton centre-of-mass energy $\sqrt{s}$ by $Q^2 = x\,y\,s$. The probability to find a parton with momentum fraction x in the proton is parametrized by parton distribution functions (PDFs), $f(x, Q^2)$.

The PDFs are an essential input for predictions of cross sections at hadron colliders like the LHC or the Tevatron. Perturbative QCD (pQCD) predicts the dependence of the PDFs on the scale Q^2, while the x dependence has to be determined from data. The kinematic coverage of various experiments in the $x - Q^2$ plane is indicated in figure 1.

Predictions of perturbative QCD can be tested in inclusive ep scattering, but also for certain hadronic final states. The production of jets is sensitive to the proton PDFs as well as the strong coupling α_S. In the production of heavy quarks like charm or bottom the mass of the heavy quark provides an additional scale for pQCD calculations. It allows tests of the treatment of several scales in the calculations and is sensitive to the heavy quark mass.

Recent measurements of electron proton and electron nucleus collisions at high energies are available from the HERA collider and the facilities at Jefferson Lab (JLAB). The

*katja.krueger@desy.de

[1]The term“electron” is used here to denote both electron and positron unless stated otherwise.

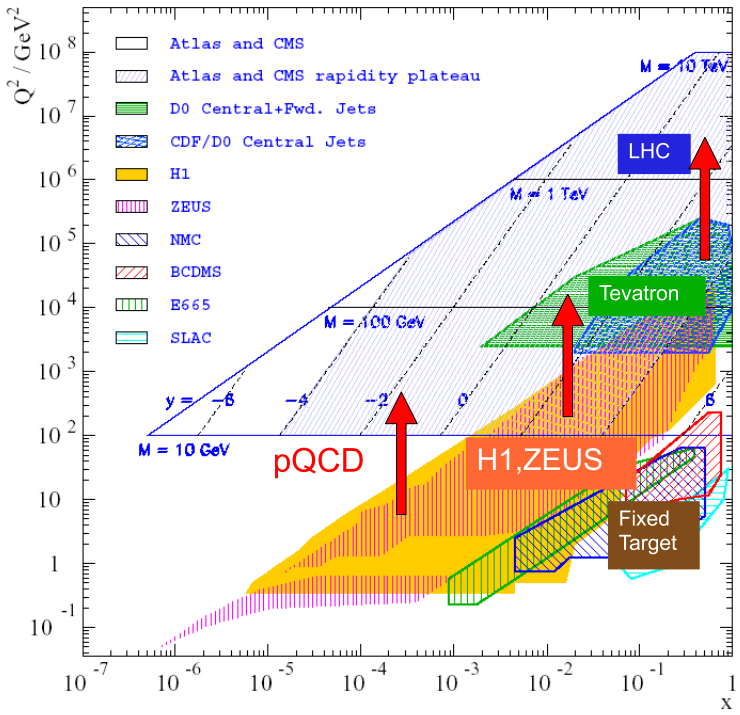

Figure 1. Kinematic coverage in proton momentum fraction x and scale Q^2 of various experiments at ep, $p\bar{p}$ and pp colliders, as well as fixed target ep experiments. The evolution in Q^2 which is predicted by pQCD is indicated by red arrows.

HERA ep collider in Hamburg was operated in the years 1992 to 2007, colliding electrons or positrons with an energy of $27.6\,\mathrm{GeV}$ and protons with an energy of $920\,\mathrm{GeV}$, at a centre-of-mass energy of $319\,\mathrm{GeV}$. The two collider experiments H1 and ZEUS collected an integrated luminosity of about $0.5\,\mathrm{fb}^{-1}$ each. The Hermes experiment used the longitudinally polarized lepton beam of HERA for scattering on polarized fixed targets, corresponding to a centre-of-mass energy per nucleon of $7.2\,\mathrm{GeV}$. At JLAB in Newport News, Virginia, the longitudinal polarized electron beam from the CEBAF accelerator with a beam energy of $6\,\mathrm{GeV}$ is used in three experimental halls for scattering on polarized fixed targets, corresponding to a centre-of-mass energy per nucleon of $3.4\,\mathrm{GeV}$. An upgrade of the beam energy to $12\,\mathrm{GeV}$ is ongoing.

2. Inclusive electron proton scattering

The most important information for the determination of the PDFs comes from electron proton scattering at virtualities $Q^2 \gtrsim 1\,\mathrm{GeV}^2$, the regime of deep-inelastic scattering (DIS). Two kinds of processes are distinguished: neutral current (NC) processes $ep \to eX$, where a photon or a Z boson is exchanged (figure 2 left), and charged current (CC) processes $ep \to \nu X$, where a W boson is exchanged (figure 2 right).

The NC cross section as a function of Q^2 and x, usually quoted in terms of the reduced

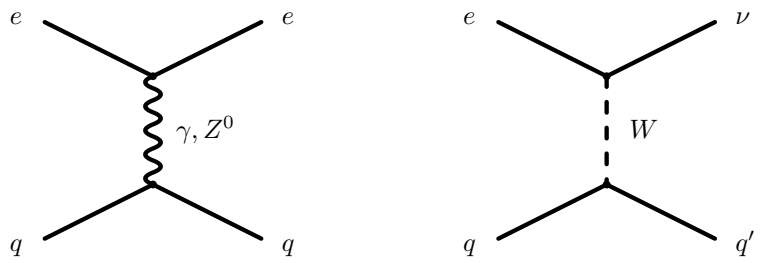

Figure 2. Schematic diagrams for the leading order neutral current (left) and charged current (right) processes in deep-inelastic electron proton scattering.

cross section $\tilde{\sigma}$, can be expressed in terms of structure functions:

$$\tilde{\sigma}^{\pm}_{\mathrm{NC}} = \frac{\mathrm{d}^2\sigma^{e^{\pm}p}_{\mathrm{NC}}}{\mathrm{d}x\mathrm{d}Q^2} \cdot \frac{Q^4 x}{2\pi\alpha^2 Y_+} = \tilde{F}_2(x,Q^2) \mp \frac{Y_-}{Y_+} x\tilde{F}_3(x,Q^2) - \frac{y^2}{Y_+}\tilde{F}_L(x,Q^2)$$
$$\text{with } Y_\pm = 1 \pm (1-y)^2,$$

where the upper sign applies to e^+p scattering and the lower sign to e^-p scattering. The dominating term comes from the structure function $\tilde{F}_2$, which in the leading order picture is proportional to the sum of the quark and antiquark densities in the proton. The contribution of $x\tilde{F}_3$ originates from the interference of the γ and Z exchange. It is proportional to the difference between quark and antiquark densities and therefore to the valence quarks. $\tilde{F}_L$ corresponds to the exchange of a longitudinally polarized photon. In the leading order picture $\tilde{F}_L = 0$, but due to higher order pQCD contributions it is approximately proportional to the product of the strong coupling α_S and the gluon density.

Due to the charge of the exchanged W boson, CC processes allow a flavour decomposition of the quark densities. In e^+p interactions, the CC cross section is mostly sensitive to the $down$-type quarks d and s, while in e^-p interactions predominantly the up-type quarks u and c take part in CC processes.

The H1 and Zeus experiments at HERA have presented combined cross section measurements of NC and CC processes with the full HERA luminosity [1]. The method [2] used for the combination of the measurements by H1 and ZEUS takes correlated uncertainties into account and leads to a cross-calibration of the two experiments. Due to this procedure the uncertainties reduce considerably more than the factor $1/\sqrt{2}$ expected from statistics. The results for the NC e^+p data are shown in figure 3. The results cover a very wide range in x from 0.00005 to 0.65 and more than four orders of magnitude in Q^2. The best precision with about 1% total uncertainty is reached in the range of medium virtualities $10 \lesssim Q^2 \lesssim 100\,\mathrm{GeV}^2$. While at medium x approximate scaling is observed, the reduced cross section rises strongly with Q^2 at small x. These scaling violations originate from gluons splitting into quark-antiquark pairs and thus provide information on the gluon density.

The combined CC reduced cross section measurement of H1 and Zeus is shown in figure 4 for e^+p and e^-p collisions. As expected from the valence quark densities dominating the large x region, the e^-p cross section that is sensitive to the up-type quarks is about twice as large as the e^+p cross section which is sensitive to the $down$-type quarks.

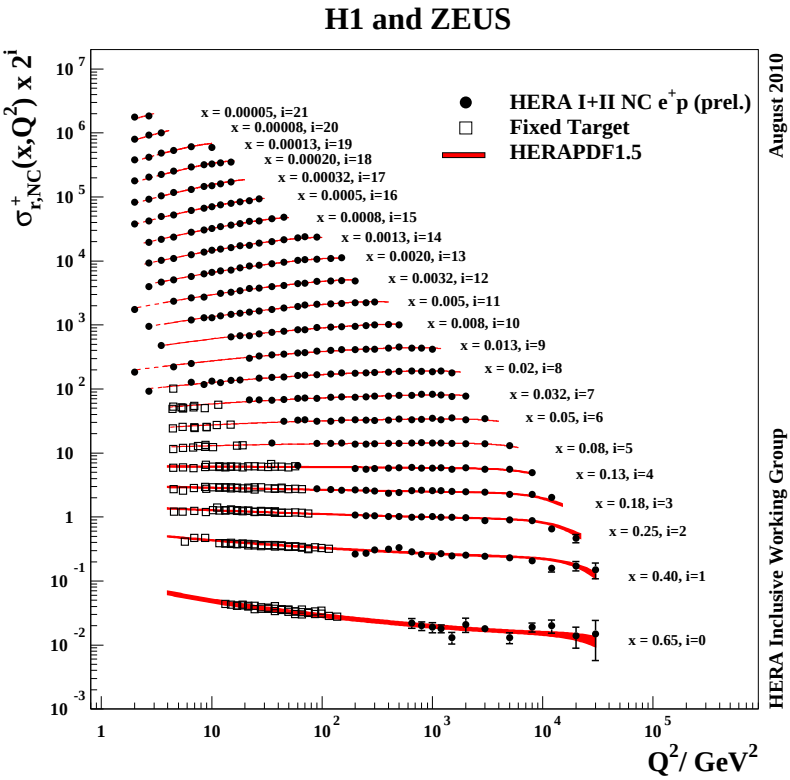

Figure 3. Combined H1 and ZEUS NC e^+p cross section measurements. Older fixed target measurements are also indicated. The data are compared to a NLO pQCD calculation using HERAPDF1.5.

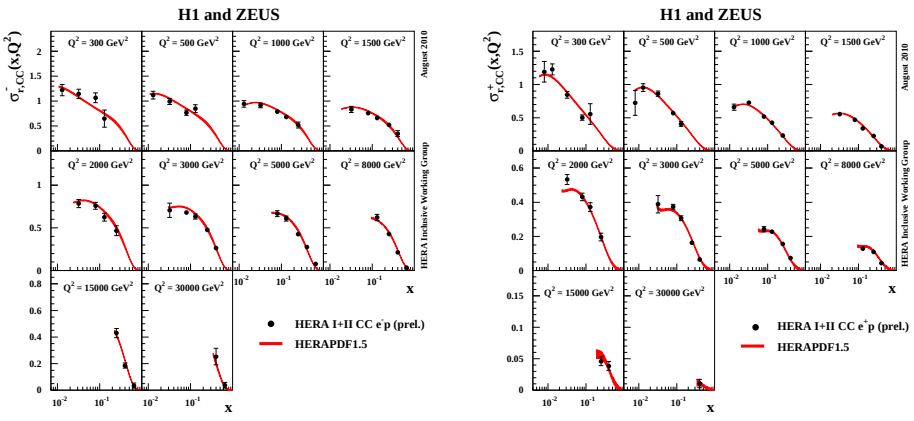

Figure 4. Combined H1 and Zeus CC e^+p (left) and e^-p (right) cross section measurements. The data are compared to a NLO pQCD calculation using HERAPDF1.5.

3. PDF fits and predictions for hadron colliders

The HERA NC and CC measurements together provide a unique, consistent data set as input for the determination of the proton PDFs. The results of PDF fits to the combined inclusive cross section data of H1 and Zeus, called HERAPDF1.5, are shown in figure 5 at next-to-leading order (NLO) and next-to-next-to-leading order (NNLO). Since only experimentally and theoretically well controlled measurements are used, a criterion of $\Delta\chi^2 = 1$ is used to determine the experimental uncertainties. Additional uncertainties due to model assumptions like the heavy quark masses and the scale Q_0^2 at which the PDFs are paramterized as well as uncertainties from the functional from chosen for the parameterization are also determined. In the medium x range, where the HERA data have very small experimental uncertainties, the PDFs are well constrained, while the PDF uncertainties grow towards small x.

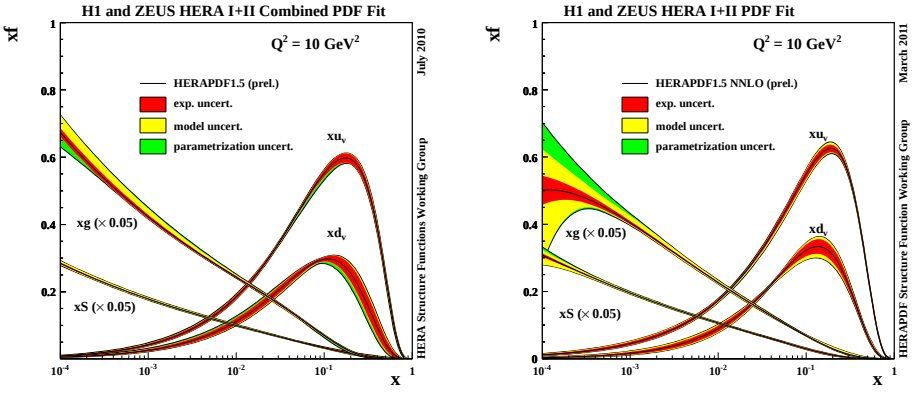

Figure 5. Summary of the proton PDF set HERAPDF1.5 determined from the full HERA combined inclusive NC and CC data at NLO [3] (left) and at NNLO [4] (right). Shown are the densities of the up (u_v) and $down$ (d_v) valence quarks, of the gluon (g) and the sea quarks (S) at a scale of $Q^2 = 10$ GeV^2. The bands show the experimental uncertainty, the uncertainty from model assumptions and from the functional from chosen for the parameterization.

The PDFs can be used to predict cross sections at the LHC like the production of jets at large transverse momentum. An example from the ATLAS Collaboration [5] is shown in figure 6. The predictions based on HERAPDF1.5 agree equally well with the measurement as PDFs determined from global fits, although no jet data were used in the determination of HERAPDF1.5.

A measurement at HERA that provides independent information on the gluon density in the proton is the structure function F_L. At the end of the HERA running the proton beam energy was reduced in order to allow a separate variation of x, y and Q^2 and thus a model-independent determination of F_L. The measurements of the H1 [6] and ZEUS [7] experiments in the region of low Q^2 are compared to pQCD predictions based on several PDFs at NLO and NNLO in figure 7. The good agreement with the data confirms the validity of the pQCD approach and the universality of the gluon PDF.

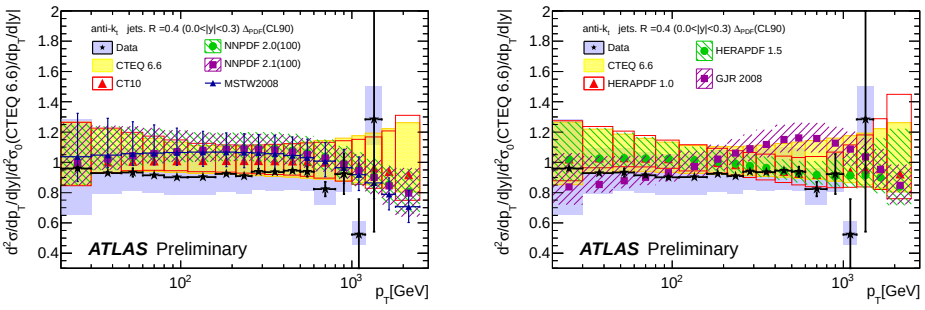

Figure 6. ATLAS measurement of the double differential jet cross section divided by the pQCD expectation based on the CTEQ6.6 PDFs as a function of the jet transverse momentum p_T. The data are compared to predictions based on several PDFs.

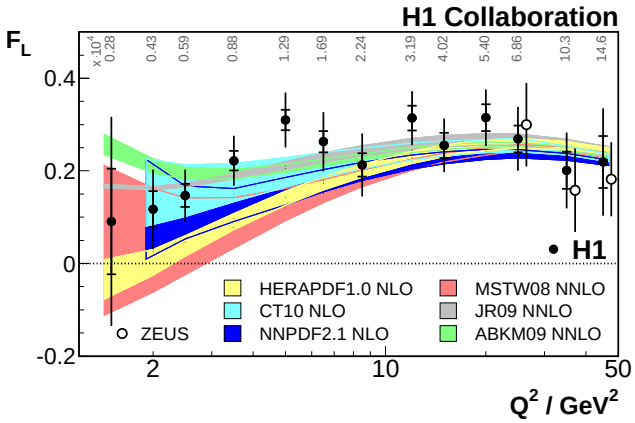

Figure 7. Measurements of the structure function F_L at low Q^2 by the H1 and ZEUS experiments. The data are compared to pQCD predictions based on different proton PDFs at NLO and NNLO.

4. Deuteron and neutron scattering

In the scattering of electrons on heavier targets in the HERMES experiment at HERA and the experiments at JLAB, the structure of heavier nuclei is studied. The scattering on deuterons allows access to the structure of the neutron which is related to the proton structure via isospin symmetry. A summary of deuteron structure function measurements from different experiments including recent results from HERMES [8] is shown in figure 8. The new data cover the transition region between the perturbative and the non-perturbative regime. They are well described by a phenomenological fit inspired by Regge theory.

In order to extract information on the neutron from the deuteron measurements, usually corrections due to the bound state have to be applied. By tagging the outgoing spectator proton and using its kinematics the BoNuS experiment in Hall B at JLAB could measure the neutron structure function F_2^n from a quasi-free neutron target in a model-independent way. The ratio of the structure functions of the neutron and the proton F_2^n/F_2^p (figure 9

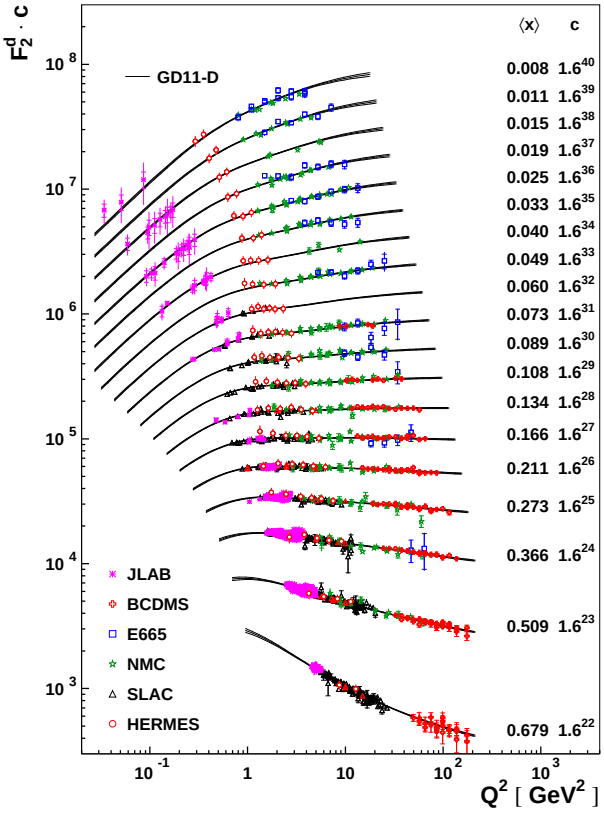

Figure 8. Summary of measurements of the inclusive structure function F_2^d for deuterons.

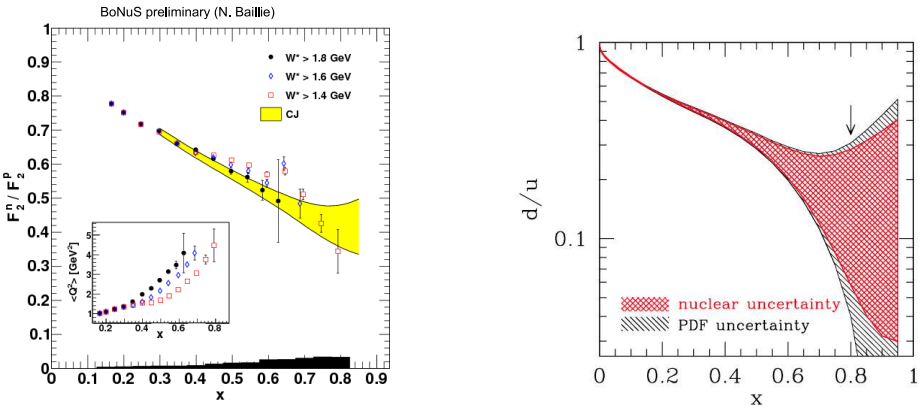

Figure 9. (left) Measurement of the ratio of the inclusive structure functions F_2^n/F_2^p of the neutron and the proton by the BoNuS experiment [9]. (right) PDF ratio d/u with uncertainties from fits of the CTEQ-JLAB collaboration [10].

left) can be used to constrain the PDF ratio d/u in the proton (figure 9 right) which up to now has large uncertainties at large x. These uncertainties result to a large extent from nuclear corrections in the determination of F_2^n.

5. Spin of the proton and generalized parton distributions

The proton has a spin of exactly $1/2$, which is rather surprising since it is a composite object. The origin of the proton spin can be studied in polarized electron proton scattering. The proton spin receives contributions from the spins of the quarks and the gluons as well as from their orbital angular momenta. It is known since long that the spins of the quarks makes up only a small fraction of the proton spin. Recent measurements of the Compass [11] and Hermes [12] experiments show that also the contribution of the gluon spin is too small to explain the total spin of the proton. The orbital angular momenta of the quarks and gluons are experimentally difficult to assess. They can be determined from integrals of the generalized parton distributions (GPDs), which take not only the longitudinal momentum but also the transverse spatial positions of the partons into account (see illustration in figure 10 left). The GPDs are a generalization of form factors, which are

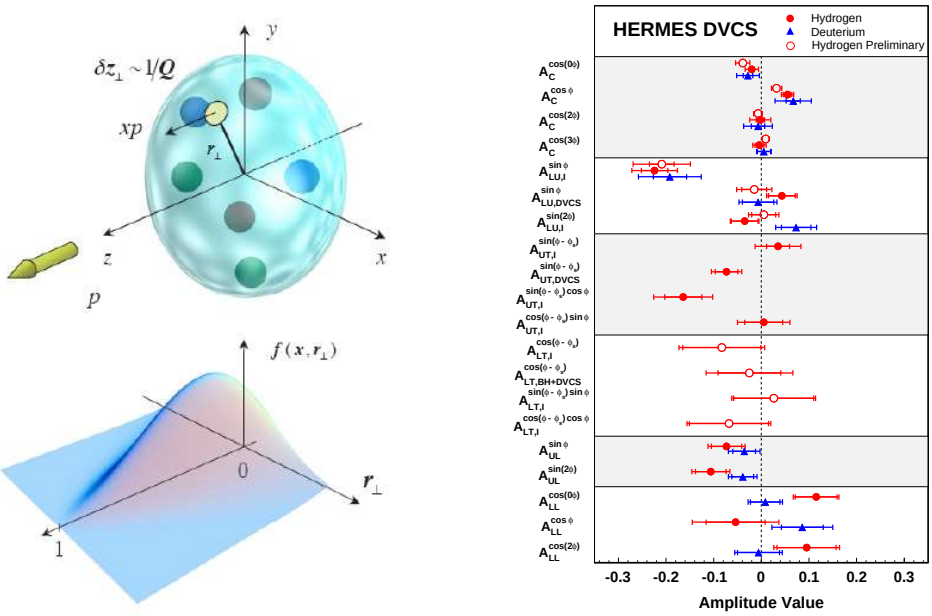

Figure 10. (left) Illustration of generalized parton distributions and their dependence on the momentum fraction x and transverse spatial position $r_\perp$ of the partons (from [13]). (right) Summary of asymmetry amplitudes for DVCS as measured by the Hermes experiment [14].

the moments of the GPDs, and PDFs, which are given by the forward limit of the GPDs. The GPDs can be determined from measurements of exclusive processes, in which the proton stays intact, like the exclusive production of vector or pseudoscalar mesons or deeply virtual compton scattering (DVCS). In order to get information on all four GPDs H, $\tilde{H}$, E and $\tilde{E}$ the asymmetries of the cross sections with respect to the beam charge, the beam spin and the target spin have to be measured. Many recent measurements of the

experiments at JLAB and of Hermes (figure 10 right) provide new information and fill in the picture of GPDs.

6. Jet production and determination of the strong coupling

Jet measurements at HERA are usually performed in the Breit frame of reference, in which the photon and the proton collide head-on. In this frame the leading order process $eq \to eq$ produces no transverse momentum, and the cross section is dominated by the QCD Compton process $eq \to eqg$, in which a gluon is radiated from the quark (figure 11 left), and the photon gluon fusion process $eg \to eq\bar{q}$, in which a gluon from the proton and the photon produce a quark-antiquark pair (figure 11 right). Therefore the jet production is directly sensitive to the strong coupling α_S and allows to disentangle α_S from the gluon density in PDF fits, while the inclusive ep cross sections are mostly sensitive to the product of α_S and the gluon density.

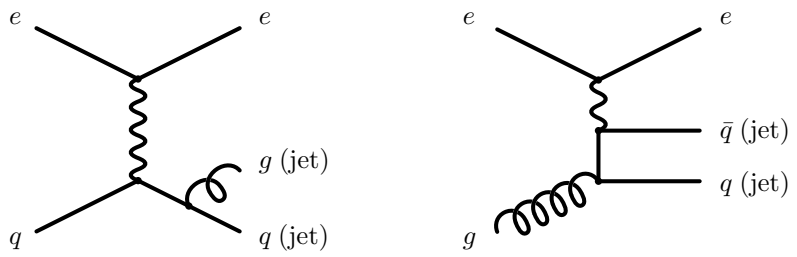

Figure 11. Schematic diagrams for the QCD Compton (left) and photon gluon fusion (right) processes in electron proton scattering.

H1 and ZEUS recently have measured the cross sections of inclusive jet production as well as of dijets and trijets [15, 16]. The dominating experimental uncertainty usually originates from the jet energy scale uncertainty, for which both experiments have reached a value of only 1%. As an example, the first double-differential cross section measurement of trijet production at large photon virtualities $150 < Q^2 < 15000\,\mathrm{GeV}^2$, measured with the H1 detector, is shown in figure 12. The data are well described by a NLO pQCD calculation using HERAPDF1.5 and $\alpha_S(M_Z) = 0.1180$. A fit to the trijet cross sections yields $\alpha_S(M_Z) = 0.1196 \pm 0.0016(exp) \pm 0.0010(pdf)^{+0.0055}_{-0.0039}(th)$ where the uncertainty is dominated by the theoretical uncertainty from missing higher orders, estimated by varying the renormalisation and factorization scale in the calculation.

Since the measurements of jet production are performed in a wide range of transverse jet energies, the cross sections are sensitive to the strong coupling in a large range of scales, and the scale dependence of α_S, the so called running, can be determined from the data of a single experiment. Both H1 and Zeus have demonstrated the running of α_S, and the results of the Zeus measurements in photoproduction ($Q^2 \simeq 0\ \mathrm{GeV}^2$) and in NC DIS are shown as an example in figure 13. The data agree between the two measurement, and they are well described by the pQCD expectation for the α_S running. The value for $\alpha_S(M_Z)$ determined from the photoproduction data is $\alpha_S(M_Z) = 0.1206^{+0.0023}_{-0.0022}(exp)^{+0.0042}_{-0.0033}(th)$, again dominated by the theoretical higher order uncertainties. The $\alpha_S(M_Z)$ values determined from jet production at HERA are compatible with the world average [17].

In order to disentangle the strong correlation between α_S and the gluon density present in fits to the inclusive HERA ep cross sections, DIS jet cross sections measured by H1 and Zeus have been included in a simultaneous fit of the PDFs and $\alpha_S(M_Z)$ [18]. The resulting PDFs are shown in figure 14 for the fit to only inclusive data (left) and to inclusive and jet data (right). The PDFs agree well, and as expected the inclusion of the jets leads to a large improvement of the uncertainty of the gluon density. The strong coupling is determined to be $\alpha_S(M_Z) = 0.1202 \pm 0.0013(exp) \pm 0.0007(param) \pm 0.0012(hadr) \pm 0.0045(scale)$, where the theoretical uncertainty is split into uncertainties related to the PDF parametrization, the hadronization of the pQCD calculation and the variation of the renormalization and factorization scale.

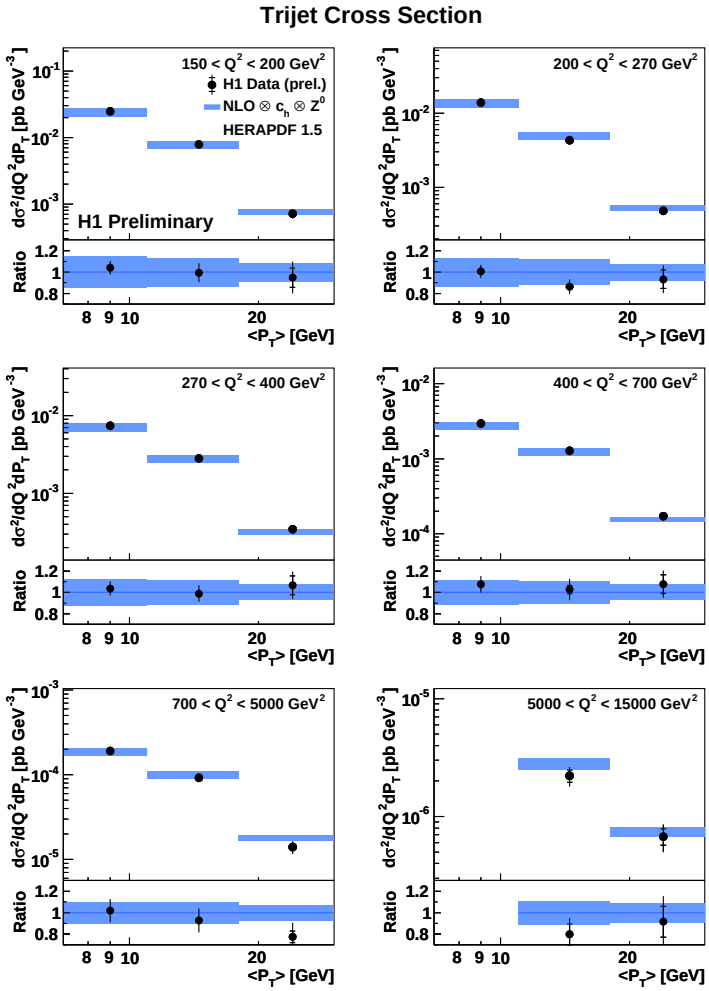

Figure 12. Double differential trijet cross sections measured with the H1 detector as a function of the photon virtuality Q^2 and the mean transverse jet momentum $\langle P_T \rangle$. In the lower parts the ratios of the data to the NLO pQCD prediction are shown.

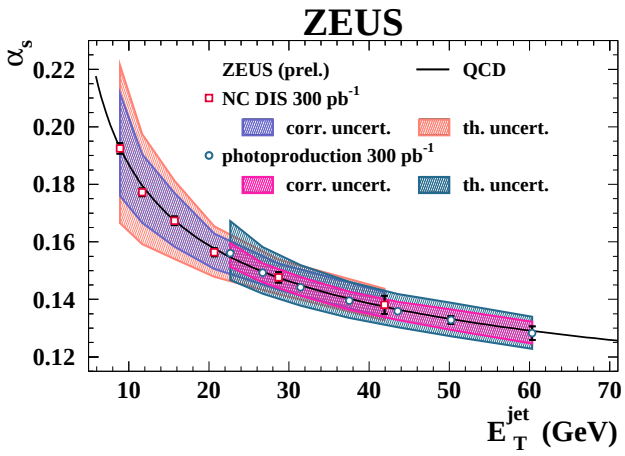

Figure 13. Running of the strong coupling α_S determined from inclusive jet cross sections measured by the ZEUS experiments in photoproduction and NC DIS as a function of the transverse jet energy.

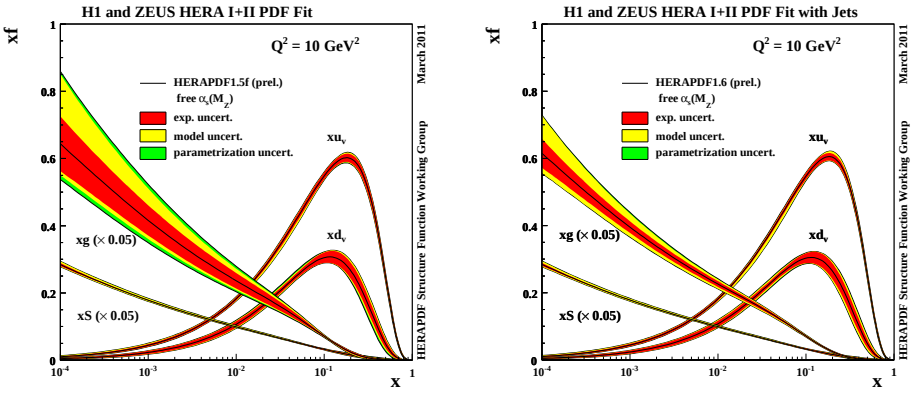

Figure 14. PDFs determined in a simultaneous fit of the PDFs and $\alpha_S(M_Z)$ to inclusive ep NC and CC cross sections (left) and to inclusive and jet cross sections (right).

7. Heavy flavour production

The production of charm and beauty quarks at HERA is dominated by the photon gluon fusion process and is therefore sensitive to the gluon density. The mass of the heavy quark provides an additional hard scale for pQCD calculations. Since charm contributes up to 30% of the inclusive ep cross section, the treatment of the heavy quark mass is important for a correct prediction also of the inclusive cross section. Measurements based on different techniques like the reconstruction of charmed mesons or the long lifetimes of the c and b flavoured hadrons can be compared by looking at the charm (beauty) contribution $F_2^{c\bar{c}}$ ($F_2^{b\bar{b}}$) to the inclusive structure function F_2. Since the H1 and ZEUS measurements of $F_2^{c\bar{c}}$ based on different experimental techniques are consistent, they are combined [19] using the same combination procedure as for the inclusive DIS cross section. The results (figure 15) reach a typical precision of $5 - 10\%$. The data are compared to predictions by pQCD calculations at NLO and NNLO employing different treatments of the charm mass and using different proton PDFs. The data are more precise than the spread of the calculations and thus can be used to constrain the theoretical predictions.

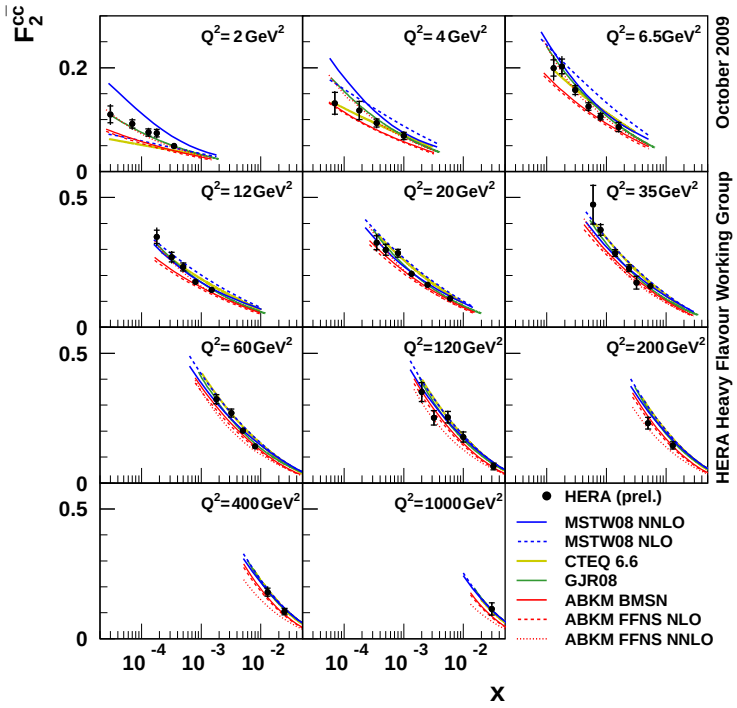

Figure 15. Combined H1 and ZEUS measurement of the charm contribution $F_2^{c\bar{c}}$ to the structure function F_2, compared to pQCD predictions.

Since the treatment of the charm mass in the pQCD calculations involves assumptions and approximations, the mass parameter m_c^{model} in a certain heavy flavour scheme ("model") does not have to agree with the physical charm mass. In fact, when the $F_2^{c\bar{c}}$ measurements together with the inclusive HERA ep cross sections are used for a simultaneous determination of the proton PDFs and m_c^{model} in several heavy flavour schemes,

different optimal values for $m_c^{\rm model}$ with minimum χ^2 are found for different schemes (figure 16 left). Since m_c has an influence of the decomposition of the sea quark density into quark flavours, it affects the cross section predictions for proton-proton collisions, for example for the production of W and Z bosons at the LHC. The dependence of the W^+ cross section predictions on $m_c^{\rm model}$ for different heavy flavour schemes, using the corresponding PDFs determined from the HERA data, is shown in figure 16 right. The predictions using the optimal $m_c^{\rm model}$ in each scheme differ by less than 2%, which is much smaller than the spread for one fixed m_c in all schemes.

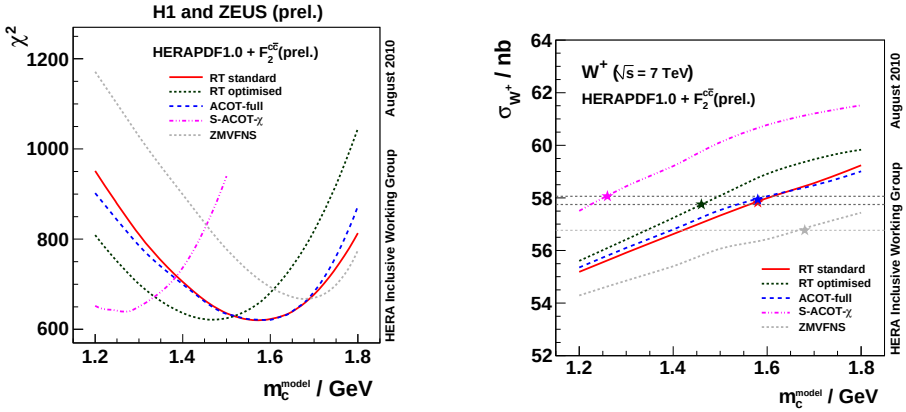

Figure 16. (left) χ^2 of the simultaneous determination of the proton PDFs and the charm mass parameter $m_c^{\rm model}$ from the HERA inclusive and $F_2^{c\bar{c}}$ data as a function of $m_c^{\rm model}$ in several heavy flavour schemes. (right) Dependence on $m_c^{\rm model}$ of the predictions of the W^+ cross section at the LHC for different heavy flavour schemes. The optimal $m_c^{\rm model}$ parameters are indicated by stars.

A simultaneous fit of inclusive NC and CC data, jet cross sections and $F_2^{c\bar{c}}$ from HERA data [21] shows that all measurements can be described by the same PDFs and that a consistent picture of the proton emerges.

8. Conclusions

Inclusive ep cross sections measured by the H1 and ZEUS experiments at HERA provide essential information on the structure of the proton and its parton content. The HERA combined measurements are a unique data set with excellent precision and cover a huge range in virtuality Q^2 and parton momentum fraction x. The PDF set HERAPDF1.5 is extracted at NLO and NNLO with the HERA inclusive cross sections as sole input. Cross section predictions by pQCD calculations based on HERAPDF1.5 give a good description of jet cross sections at the LHC.

The origin of the spin of the proton is studied in polarized electron-proton and electron-nucleus scattering in experiments at JLAB and the Hermes experiment at HERA. Generalized parton distributions, which are accessible in DVCS, contain information on the contribution of the orbital angular momenta of quarks and gluons to the proton spin.

Measurements of the hadronic final state in ep collisions like cross sections for the production of jets or of heavy quarks provides not only a testing ground for pQCD predictions, but also additional information on the proton structure and access to other quan-

tities. Jet production allows a precise determination of the strong coupling α_S and its running, as well as a possibility to disentangle the correlation between α_S and the gluon density that is present in inclusive ep cross sections. The measurements of heavy quarks are sensitive to the quark mass and its treatment in pQCD calculations.

Acknowledgements

I am grateful to Naba Mondal, Rohini Godbole and all the other organizers of Lepton-Photon 2011 for inviting me and giving me the opportunity to participate in this very interesting and well organized conference in a fascinating place.

References

[1] H1 and ZEUS Collaboration, *H1prelim-10-141/ZEUS-prel-10-017*.
[2] F.D. Aaron *et al.* [H1 and ZEUS Collaboration], *JHEP* **1001**, 109 (2010) [arXiv:0911.0884].
[3] H1 and ZEUS Collaboration, *H1prelim-10-142/ZEUS-prel-10-018*.
[4] H1 and ZEUS Collaboration, *H1prelim-11-042/ZEUS-prel-11-002*.
[5] ATLAS Collaboration, *ATL-PHYS-PUB-2011-005*.
[6] F.D. Aaron *et al.*, *Eur. Phys. J. C* **71**, 1579 (2011) [arXiv:1012.4355].
[7] S. Chekanov *et al.* [ZEUS Collaboration], *Phys. Lett. B* **682**, 8 (2009) [arXiv:0904.1092].
[8] A. Airapetian *et al.* [HERMES Collaboration], *JHEP* **1105**, 126 (2011) [arXiv:1103.5704].
[9] S. Tkachenko (for the CLAS Collaboration), "Model-independent extraction of neutron structure functions from deuterium data," Proceedings of the DIS2011 Conference, Newport News, Virginia
[10] A. Accardi *et al.* [CTEQ-JLAB Collaboration], *Phys. Rev. D* **84**, 014008 (2011) [arXiv:1102.3686].
[11] E.S. Ageev *et al.* [COMPASS Collaboration], *Phys. Lett. B* **633**, 25 (2006) [hep-ex/0511028]; M. Alekseev *et al.* [COMPASS Collaboration], *Phys. Lett. B* **676**, 31 (2009) [arXiv:0904.3209].
[12] A. Airapetian *et al.* [HERMES Collaboration], *JHEP* **1008**, 130 (2010) [arXiv:1002.3921].
[13] A.V. Belitsky and A.V. Radyushkin, *Phys. Rept.* **418**, 1 (2005) [hep-ph/0504030].
[14] HERMES Collaboration, preliminary, HERMES transparencies 11-004a
[15] H1 Collaboration, *H1prelim-11-032*;
F.D. Aaron *et al.* [H1 Collaboration], *Eur. Phys. J. C* **67**, 1 (2010) [arXiv:0911.5678];
F.D. Aaron *et al.* [H1 Collaboration], *Eur. Phys. J. C* **65**, 363 (2010) [arXiv:0904.3870].
[16] ZEUS Collaboration, *ZEUS-prel-11-005*;
ZEUS Collaboration, *ZEUS-prel-10-014*;
ZEUS Collaboration, *ZEUS-prel-10-002*;
H. Abramowicz *et al.* [ZEUS Collaboration], *Eur. Phys. J. C* **70**, 965 (2010) [arXiv:1010.6167].
[17] S. Bethke, *Eur. Phys. J. C* **64**, 689 (2009) [arXiv:0908.1135].
[18] H1 and ZEUS Collaboration, *H1prelim-11-034/ZEUS-prel-11-001*.
[19] H1 and ZEUS Collaboration, *H1prelim-09-171/ZEUS-prel-09-015*.
[20] H1 and ZEUS Collaboration, *H1prelim-10-143/ZEUS-prel-10-019*.
[21] H1 and ZEUS Collaboration, *H1prelim-11-143/ZEUS-prel-11-010*.